ADVANCED NANOBIOMED RESEARCH
www.advnanobiomedres.com

Liquid Biopsy beyond Cancer: A miRNA Detection in Serum with Electrochemical Chip for Non-Invasive Coeliac Disease Diagnosis

Veronica Caratelli, Maria Moccia, Francesca R. Paggioro, Luca Fiore, Concetta Avitabile, Michele Saviano, Anna Lisa Imbriani, Principia Dardano, Luca De Stefano, Danila Moscone, Nicola A. Colabufo, Imane Ghafir El Idrissi, Francesco Russo, Giuseppe Riezzo, Gianluigi Giannelli, and Fabiana Arduini**

Coeliac disease is a very common autoimmune disease estimated to affect 1 in 100 people worldwide. It occurs in genetically predisposed people where the ingestion of gluten leads to damage in the small intestine, and it is accurately diagnosticated through duodenal biopsy, an invasive diagnostic method. The liquid biopsy, generally used for monitoring cancer, is an appealing alternative even for autoimmune pathology such as coeliac disease, allowing for detecting disease progression or resistance to treatment. For this reason, an electrochemical peptide nucleic acid (PNA) device combined with a smartphone-assisted potentiostat for non-invasive coeliac disease diagnosis is proposed, by measuring the selected overexpressed miRNA-486-5p in serum, enlarging the application of liquid biopsy in nontumor pathologies. For highly sensitive detection, the polyester-based printed sensor is nanomodified with gold nanoparticles and a synthetic customized PNA probe. The designed sensor can detect the target analyte in the range of 10–100 nM with a limit of detection of 0.7 nM by measuring the variation of the response of the electrochemical mediator hexaammineruthenium in the presence of PNA–miRNA duplex on the nanostructured working electrode surface. The analyses testing serum samples are found in agreement with ones obtained by real-time quantitative polymerase chain reaction (RT-qPCR), demonstrating the reliability of this innovative electrochemical chip developed.

1. Introduction

Coeliac disease (CD) is one of the most common autoimmune disorders affecting many people in the Western world. The onset of this enteropathy is triggered by the common protein fraction of wheat flour, namely gluten, in people with a genetic predisposition carrying human leukocyte antigen DQ2 and DQ8 haplotypes.[1] The symptoms encompass abdominal pain, diarrhea, and weight loss[2,3] due to the flattened small intestinal mucosa with a lymphocytic infiltrate, crypt hyperplasia, and villous atrophy.[4] The average occurrence of this disease is reported in a population of between 0.5% and 1% worldwide,[5,6] with a prevalence of CD in patients affected by other conditions, including insulin-dependent diabetes mellitus type 1, autoimmune thyroid disease, inflammatory bowel disease, and irritable bowel syndrome (IBS).[7,8] The CD diagnosis starts with the search of immunoglobulin A antibodies, tissue transglutaminase 2,

V. Caratelli, F. R. Paggioro, L. Fiore, D. Moscone, F. Arduini
Department of Chemical Science and Tecnologies
University of Rome "Tor Vergata"
Via della Ricerca Scientifica, 00133 Rome, Italy
E-mail: fabiana.arduini@uniroma2.it

M. Moccia, C. Avitabile, M. Saviano
Institute of Crystallography
National Research Council (CNR)
Via G. Amendola 122/O, 70126 Bari, Italy
E-mail: maria.moccia@cnr.it

The ORCID identification number(s) for the author(s) of this article can be found under https://doi.org/10.1002/anbr.202200015.

© 2022 The Authors. Advanced NanoBiomed Research published by Wiley-VCH GmbH. This is an open access article under the terms of the Creative Commons Attribution License, which permits use, distribution and reproduction in any medium, provided the original work is properly cited.

DOI: 10.1002/anbr.202200015

A. L. Imbriani
Biochemical Systems International S.p.A.
Loc, Palazzo del Pero, 23, 52100 Arezzo, Italy

P. Dardano, L. De Stefano
Department of Physical Sciences and Matter Technology
Institute for Applied Science and Intelligent Systems
National Research Council
Via Pietro Castellino 111, 80131 Napoli, Italy

N. A. Colabufo, I. Ghafir El Idrissi
Department of Pharmacy-Pharmaceutical Science
University of Bari Aldo Moro
Via Orabona 4, 70125 Bari, Italy

N. A. Colabufo, I. Ghafir El Idrissi
Biofordrug S.R.L
Spin-off of the University of Bari Aldo Moro
Via Dante 99, Triggiano, 70019 Bari, Italy

and the endomysial IgA antibody in the blood, boosting the identification of patients who undergo an endoscopic biopsy. Despite the high sensitivity of the biochemical analyses, no currently available analysis in serum provides enough sensitivity and specificity; therefore, a duodenal biopsy is required.[9] Indeed, the current recommendations established the duodenal biopsy as the gold-standard method for the accurate diagnosis of this enteropathy,[10] though it is an invasive diagnostic method. In the case of cancer, even if the tumor tissue remains the gold-standard source for clinical molecular analyses, the monitoring of cancer-derived material circulating in the bloodstream, called liquid biopsy, has become an appealing alternative. The high potential of this diagnostic technique has also been recognized at a worldwide level, being listed in 2017 among the Top 10 Emerging Technologies.[11] The advantage of a liquid biopsy is not only related to the lack of invasiveness, but it also allows to detect the disease at an early stage. Furthermore, the tissue biopsies examine only selected bits of tumors and can miss cells that have turned more dangerous than their neighboring cells have. The overall potential of liquid biopsy is its capability to detect the full spectrum of mutations, indicating when a more aggressive treatment is needed, furnishing a fast and easy test for diagnosis and prognosis of cancer. The application of a liquid biopsy for other autoimmune pathologies is also emerging as a potential diagnostic tool for CD. Therefore, considering that the tissue biopsy is the gold-standard method for both cancer and CD, herein, we investigated the expression of selected miRNA in the serum of CD patients. Currently, in the literature, only a few articles reported miRNAs expression in patients with CD, mainly evaluated in the intestinal mucosa.[12–14] MicroRNAs (miRNAs) have been found circulating in different body fluids, such as serum and plasma, protected by a protein binding or enclosed in vesicles and released in the extracellular space.[15] Circulating miRNAs represent reliable and promising diagnostic, prognostic, and therapeutic biomarkers, because miRNAs modulate >30% of mammalian genes and participate in almost all known cellular processes, including development, DNA repair, cell cycle regulation, differentiation, apoptosis, as well as malignant cellular transformation and host–pathogen interaction.[16,17] To this regard, Bascunan et al. reported the first description of an altered pattern of inflammation-related miRNA expression in blood immune cells and plasma in CD adult patients. They evaluated the expression levels of miRNA-146a, miRNA-155, and miRNA-21 in peripheral blood mononuclear cells, miRNA-155 in monocytes, and miRNA-155, miRNA-21, and miRNA-125b in plasma of CD patients using TaqMan microRNA Reverse Transcription Kit, suggesting their participation in the immune processes underlying this pathology.[18] However, despite the huge potential for miRNAs in the diagnosis and prognosis of cancer, the current detection approaches are generally confined to classical nucleic acid detection methods such as northern blotting, microarray, quantitative real-time quantitative polymerase chain reaction ((*q*)RT-PCR), and next-generation sequencing.[19]

In the overall scenario of smart analytical methods for miRNA detection, the biosensors have demonstrated several advantages including the cost-effectiveness of the analyses, the miniaturization of the device, and the capability to work in complex matrix.[20,21] Among the different transducers, the electrochemical one has revealed its potential to address the challenges related to the detection of circulating nucleic acids such as the low detection limit in clinical samples.[22] For example, Tavallaie et al. proposed a novel approach based on an electric-field-induced reconfiguration of labeled DNA-modified gold-coated magnetic nanoparticles to detect miRNA-21 expression level directly in whole blood, with high sensitivity within the concentration range of 10 aM–1 nM.[23] Yuan's group developed a gallium zinc oxide field-effect transistor (IGZO FET) for the detection of miRNA-21 in human urine as a trace bladder cancer-associated biomarker. Considering the uniform and smooth structure of IGZO with excellent electrical performance, the single-stranded DNA-functionalized IGZO FET exhibited high sensitivity with an ultralow detection limit of 19.8 aM.[24]

Umer et al. designed a novel amplification-free sandwich-type platform assay for electrochemical detection of miRNA-DNA chimera by using HRP-labeled p53 able to bind the recognition sequence. The amperometric signal was monitored in presence of hydroquinone and H_2O_2, obtaining a limit of detection equal to 22 fM.[25]

Shiddiky's research group developed different amplification-free electrochemical approaches for the detection of miRNA using screen-printed gold electrodes. The first device relies on gold-loaded nanoporous superparamagnetic iron oxide nanocubes for the detection of miRNA-107 (Au–NPFe_2O_3NC). The target miRNA was directly adsorbed onto the gold surfaces of Au–NPFe_2O_3NC via gold-RNA affinity interaction. The electrocatalytic activity of Au–NPFe_2O_3NC was then used for the reduction of ruthenium hexaammine(III) chloride bound with target miRNA. The catalytic signal was further amplified by using the ferri/ferrocyanide electroactive probe. These multiple signal enhancement steps enable this device to achieve the detection limit of 100 aM.[26] The second sensor was developed for the detection of FAM134B mRNA which was selectively isolated by magnetic separation and adsorbed directly onto an unmodified gold-screen-printed electrode (gold-SPE). The surface-attached miRNA was measured by differential pulse voltammetry in the presence of $[Fe(CN)_6]^{4-/3-}$ redox system. This method demonstrated good sensitivity, with a limit of detection equal to 1.0 pM and reproducibility with relative standard deviation (RSD%) = <5%, for $n = 3$.[27] Following the improvement of biosensors using nanomaterials, the new frontiers of e-devices have been oriented toward miniaturization and portability since the healthcare trend is changing toward becoming more patient oriented. To this aim, the development of electrochemical devices by combining screen-printed electrodes and smartphone technology has allowed obtaining more suitable instruments to be applied in healthcare diagnostics, acting as a portable and convenient platform for point-of-care testing (POCT). In this regard, Low et al. developed a smartphone-based

F. Russo, G. Riezzo, G. Giannelli
National Institute of Gastroenterology "S. de Bellis"
Research Hospital
Castellana Grotte, 70013 Bari, Italy

F. Arduini
SENSE4MED S.R.L.
Via della ricerca scientifica, 00133 Rome, Italy

© 2022 The Authors. Advanced NanoBiomed Research published by Wiley-VCH GmbH

biosensing system composed of a disposable screen-printed biosensor modified with reduced graphene oxide/gold composite, to detect salivary circulating miRNA-21. The hybridization between the miRNA-21 targets and ssDNA probe on the rGO/Au-modified electrode resulted in the decrease in peak current with the increase in miRNA-21 target concentration. The smartphone-based biosensing system showed comparable performance with a commercial electrochemical workstation for miRNA-21 detection in the concentration range of 1×10^{-4}–1×10^{-12} M.[28]

Herein, we developed a smartphone-assisted electrochemical chip based on label-free detection for non-invasive CD diagnosis, by exploiting the interaction of the positive charge of the electrochemical probe hexaammineruthenium with the well-known different charges of peptide nucleic acid (PNA) and miRNA.[29,30] First, we investigated the following four miRNAs involved in the onset of CD: miRNA-449a (5' UGGCAGUGUAUUGUUAGCUGGU 3'), miRNA-492 (5' AGGACCUGCGGGACAAGAUUCUU 3'), miRNA-21-5p (5' UAGCUUAUCAGACUGAUGUUGA 3'), miRNA-486-5p (5' UCCUGUACUGAGCUGCCCCGAG 3'), selecting the miRNA useful for the diagnosis of CD. Subsequently, the selected miRNA-486-5p was employed to develop the electrochemical chip using a complementary PNA sequence as a molecule probe to realize an innovative and sustainable sensing tool for non-invasive CD diagnosis (**Figure 1**).

2. Results and Discussion

2.1. Patients Cohort Analysis

Cases for the present study were recruited from among the outpatients of the National Institute of Gastroenterology "S. de Bellis" Research Hospital, Castellana G. (Italy). CD

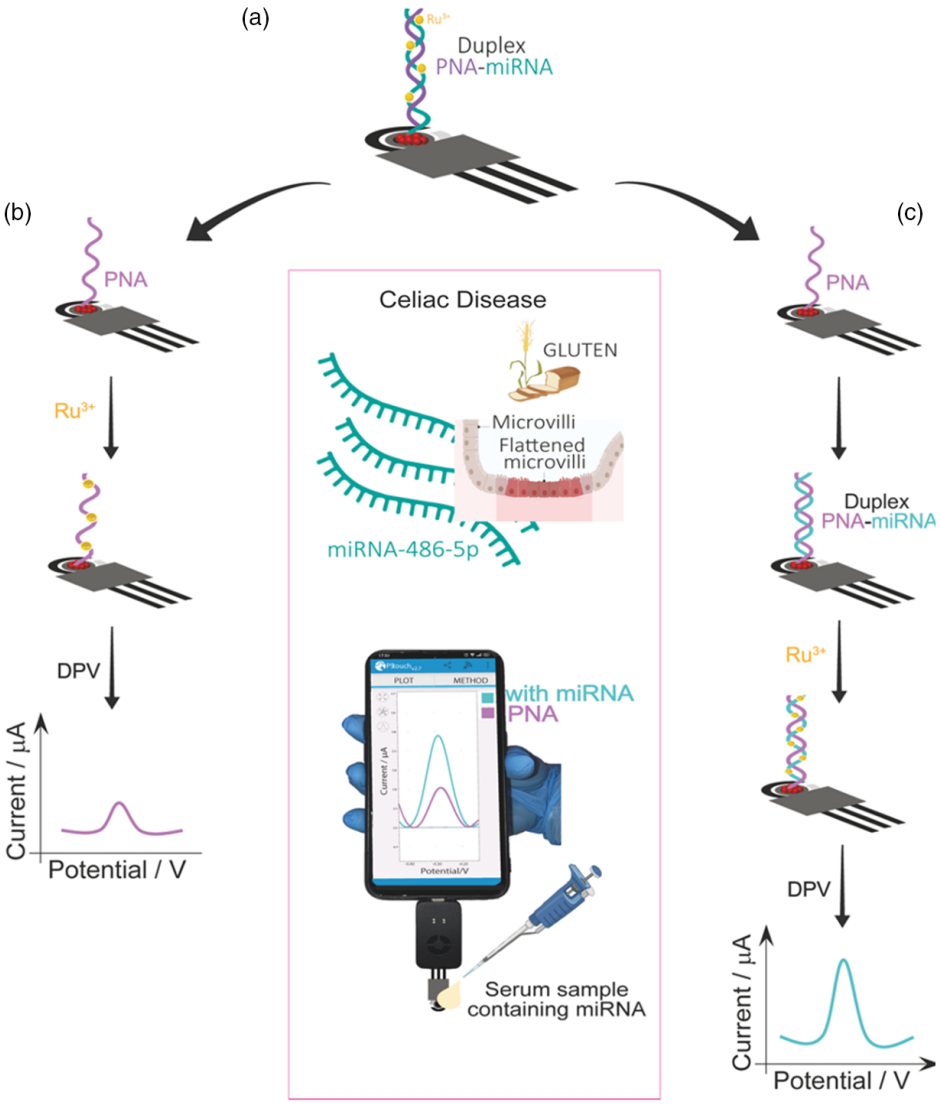

Figure 1. Electrochemical detection of miRNA-486-5p using the smartphone-assisted peptide nucleic acid (PNA)-based printed electrochemical biosensor. Picture of the laboratory setup consisting of a screen-printed electrode a) connected to the miniaturized potentiostat Sensit Smart connected to a smartphone. b) Measurement of the blank signal. c) Measurement of miRNA-486.

© 2022 The Authors. Advanced NanoBiomed Research published by Wiley-VCH GmbH

patients were diagnosed based on positive antiendomysium antibodies (EMAs) and antitransglutaminase antibodies (TGAs). Biopsies from the proximal part and the distal part of the duodenum were taken to confirm the diagnosis according to the modified Marsh–Oberhuber criteria (grades 3b–3c).[31] After the diagnosis, CD patients followed a specific gluten-free diet (GFD) and received additional counseling at follow-up. Patients with CD were evaluated at the time of diagnosis and at least 12 months after the start of GFD. The dietary compliance assessment at the 1-year checkup was based on an examination consisting of a physical exam, the patient's self-reported compliance, and the doctor's opinion.

As for the IBS patient group, the IBS patients with diarrhea were enrolled according to the description of Longstreth et al.[32] Only the HLA-DQ2/HLA-DQ8 negative/negative IBS patients were considered for this study, because gluten-sensitive diarrhea without CD is a clinical entity that has been seen in IBS patients positive for HLA-DQ2 or HLA-DQ8.[33]

Healthy control (HC) subjects were enrolled among the administrative staff of "S. de Bellis" Research Hospital. They reported not having metabolic, endocrine, or immunological diseases, dyspepsia, or other gastrointestinal (GI) diseases and were not taking any medication. Information on the health status of subjects was obtained during an examination consisting of a physical exam and an interview on their current lifestyle, diet, and medical history. As criteria for admission, EMA and TGA had to be negative. Moreover, metabolic parameters (blood glucose, HbA1c, lipid profile, body weight, and blood pressure) had to be in the normal range of values. This research was conducted according to the guidelines stipulated in the Declaration of Helsinki and all procedures involving human subjects and patients had been approved by the local Science and Ethics Committee. Written informed consent was obtained from all the patients and healthy subjects. This clinical trial had been registered at http://www.clinicaltrials.gov (registration number NCT01574209). Overall, the expression patterns of miRNAs were tested in the serum of a cohort of 12 patients with CD (1 man and 11 women, mean age 32 ± 11) before and after 1 year of a GFD, 14 IBS patients (1 man and 13 women, mean ages 39 ± 15), and 14 healthy volunteers (HC) (4 men and 10 women, mean ages 38 ± 14) (number of samples = 52). The quantitative analysis of the miRNAs through the RT-PCR technique is described in the Experimental Section.

All the 40 recruited subjects underwent a blood sampling to evaluate their blood chemistry parameters. All serum data were within the normal range. Worthy of note, IgA-endomysial antibody (EMA IgA) and IgA-transglutaminase antibody (tTG IgA) were not detectable in IBS patients and control subjects (**Table 1**).

For the 12 CD patients, clinical serum data were collected before and after one year of GFD, and the results are reported in **Figure 2**. Once CD patients started the GFD, both EMA IgA and t-Tg IgA dramatically decreased compared to initial values, thus indicating an optimal response to gluten restriction.[34]

The collection of human serum samples has been carried out by a medical doctor from a colleague, following ethical guidelines provided by occupational health section, University of Oxford.[35] We supplied the Donor Information Sheet and Donor Consent form to the donor.

2.2. Analysis of miRNA Expression

All 40 samples were analyzed, and each subject was tested for each of the miRNAs considered: miRNA-39-3p, miRNA-16-5p, miRNA-449a, miRNA-492, miRNA- 21-5p, and miRNA-486-5p. In addition, samples from CD patients under GFD were also investigated to detect if any variation in miRNA expression profile occurs before and after the elimination of gluten from the diet. Furthermore, the analysis of samples from IBS patients can permit the evaluation of differences in terms of miRNAs expression in the two diseases. For miRNA-39-3p, a relatively constant expression was shown in all four groups of subjects analyzed (CD patients, CD patients after 1 year of GFD, IBS patients, and healthy cases) with an average Ct value of about 27. This data confirms that the extraction of miRNAs was efficient and constant in the various samples.

miRNA-449a and miRNA-492 were not detected in any of the samples analyzed; therefore, from evaluating the first data obtained, we can assume that they are not present at detectable concentrations in serum.

miRNA-21-5p and miRNA-486-5p were detected in all the samples analyzed: HCs, CD patients at baseline, CD patients under GFD, and patients with IBS. The expression of miRNA-21-5p and miRNA-486-5p are represented both as a function of Ct and $2^{-\Delta\Delta CT}$ ratio in **Figure 3**.

As represented in Figure 3a, miRNA-21-5p exhibits a rather late Ct in all 4 biological groups analyzed (CTRL 32.6 ± 0.1; CD 32 ± 0.04; GFD 32.5 ± 0.2; IBS 33.5 ± 0.2). In CD patients, the Ct value is lower than in the other groups; therefore, the expression is slightly higher than in HCs, GF diet patients, and IBS patients. In particular, as shown in Figure 3b, miRNA-21-5p is 1.6 ± 0.1 fold over-expressed in coeliac patients

Table 1. Clinical serum data of recruited cohort.

Cohort	Glu[a)]	Tag[b)]	Ferr[c)]	RBC[d)]	Leu[e)]	Hb[f)]	Hct[g)]	Plt[h)]	Ast[i)]	Alt[i)]
CD	87 ± 2.8	95 ± 8	27 ± 8	4.5 ± 0.14	6.6 ± 0.6	13 ± 0.4	39 ± 1	252 ± 21	19 ± 5	25 ± 8
IBS	87 ± 2.6	91 ± 10	48 ± 12	4.6 ± 0.16	9.9 ± 3.5	14 ± 0.2	41 ± 0.8	245 ± 14	15 ± 1.6	23 ± 3
Controls	84 ± 1.6	118 ± 19	53 ± 16	4.7 ± 0.13	5.8 ± 0.3	14 ± 0.3	41 ± 1	257 ± 25	19 ± 2	27 ± 2.7

[a)]Glu = glucose (mg dL^{-1}); [b)]Tag = triacylglycerol (mg dL^{-1}); [c)]Ferr = ferritin (μg L^{-1}); [d)]RBC = red blood cells ($\times 10^3$ μL^{-1}); [e)]Leu = leucocytes (10^3 μL^{-1}); [f)]Hb = hemoglobin (g dL^{-1}); [g)]Hct = hematocrit (%); [h)]Plt = number of platelet ($\times 10^3$ μL^{-1}); [i)]Ast = aspartate aminotransferase (IU L^{-1}); [i)]Alt = alanine aminotransferase (IU L^{-1}).

© 2022 The Authors. Advanced NanoBiomed Research published by Wiley-VCH GmbH

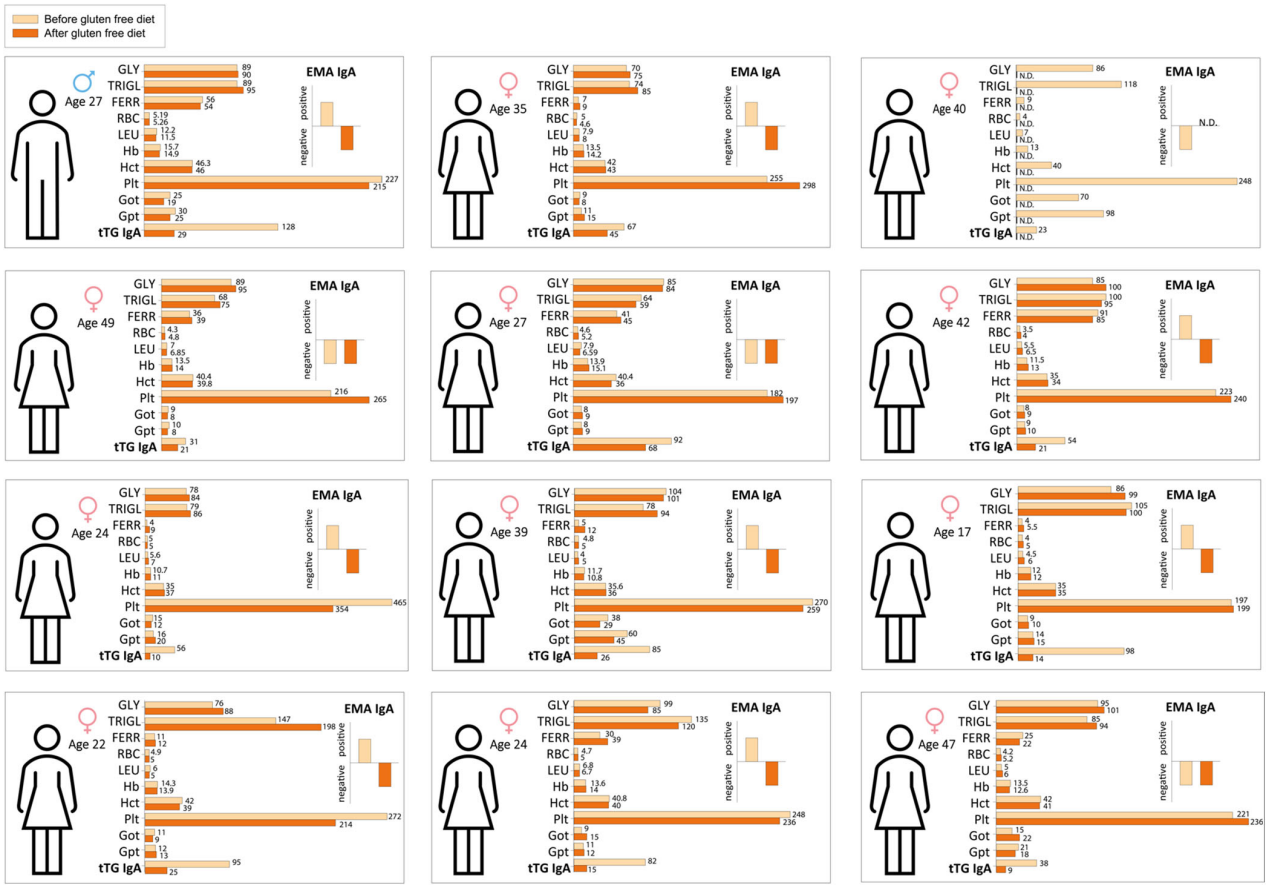

Figure 2. Clinical serum results of 12 coeliac patients before and after gluten-free diet.

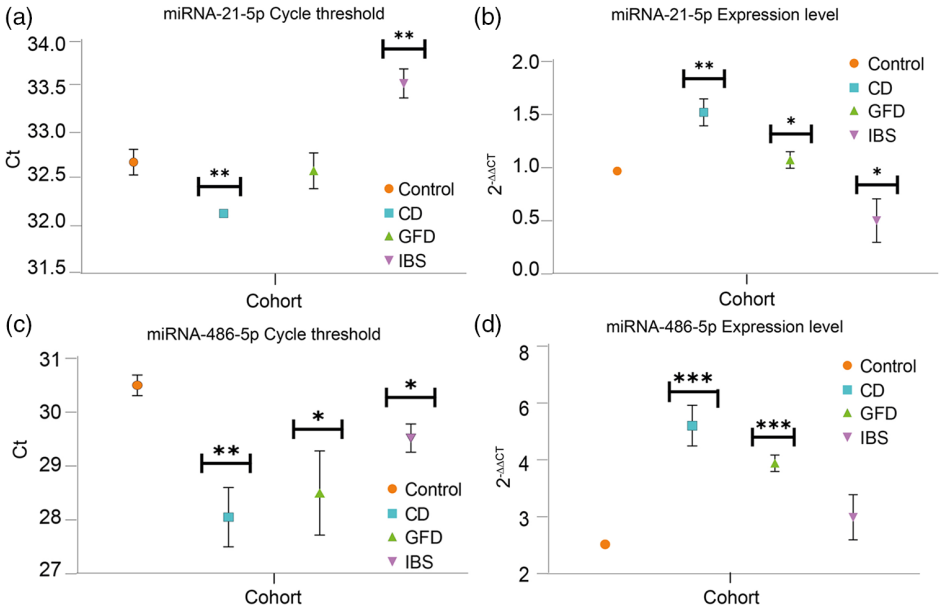

Figure 3. miRNA-21-5p and miRNA-486-5p expression in four cohorts: control, coeliac disease patients, patients under gluten-free diet, and patients with irritable bowel syndrome. a) Cycle threshold of miRNA-21-5p in all recruited subjects subdivided into four groups. b) Over-expression of miRNA-21-5p in all cohorts with respect to controls. c) Cycle threshold of miRNA-486-5p in all recruited subjects subdivided into four groups. d) Over-expression of miRNA-486-5p in all cohorts with respect to controls. For miRNA analysis in a real-time polymerase chain reaction (PCR), each sample of serum was tested in triplicate ($n = 3$) and data expressed as mean ± standard deviation (SD). Statistical significance using one-way analysis of variance (ANOVA) with $P < 0.05$ in comparison with control group and $^{*}P < 0.1$, $^{**}P < 0.01$, $^{***}P < 0.001$ pathological group, with unpaired t-test.

 © 2022 The Authors. Advanced NanoBiomed Research published by Wiley-VCH GmbH

compared with controls. Even in CD patients after 1 year of GFD, miRNA-21-5p is over-expressed about 1.1 ± 0.1 fold with respect to controls, while IBS patients revealed an under-expression of this miRNA compared to the healthy population with a $2^{-\Delta\Delta CT}$ ratio of 0.5 ± 0.2.

miRNA-486-5p presented earlier Ct (CTRL 30.5 ± 0.2; CD 28 ± 0.6; GFD 28.5 ± 0.8; IBS 29.5 ± 0.3) in the analyzed cohorts and in particular in the coeliac group. In CD patients, miRNA-486-5p was over-expressed compared to HCs, CD patients after GFD, and IBS patients, too. In particular, as shown in Figure 3d, in CD patients, miRNA-486-5p is 5 ± 1 fold over-expressed with respect to controls, in CD patients after GFD, the expression is greater 3.9 ± 0.3 fold compared to HC, and in IBS patients, the expression of miRNA-486-5p is 1.7 ± 0.9 fold higher compared to healthy subjects.

In conclusion, the data obtained suggest that miRNA-21-5p and miRNA-486-5p are over-expressed in CD patients compared to healthy subjects, and the over-expression is also higher than that in CD patients after GFD and IBS patients. Furthermore, miRNA-486-5p exhibits a higher level of expression in blood than miRNA-21-5p; therefore, it may be considered a more suitable marker for CD, helpful in developing a panel to introduce in the clinical practice.

Noteworthy, our data suggest that following the expression level of both miRNAs, it seems that there is a return to levels similar to those of HC.

2.3. Electrochemical and Morphological Platform Characterization

After demonstrating the suitability of miRNA-486-5p as a suitable biomarker for CD, we developed the electrochemical PNA-based chip capable of detecting the specific miRNA sequence in serum samples. In detail, the sensor is composed of a graphite-based working electrode and counter electrode combined with a silver/silver chloride pseudo-reference electrode. The miRNA-486-5p detection was carried out using a signal on a method based on the detection of the electrochemical mediator hexaamminerutheninum added to the working solution for monitoring the PNA-miRNA duplex formation.[36] The positively charged $Ru(NH_3)_6^{3+}$ is accumulated at the working electrode through electrostatic interaction with the negatively charged miRNA, allowing for an increase of the signal current due to the formation of PNA–miRNA duplex, being the PNA oligomer uncharged (Figure 1).

The biosensor performance depends directly on the success of device fabrication steps, namely drop-casting of AuNPs on an electrode surface, PNA immobilization, and PNA-miRNA hybridization step. For this reason, atomic force microscopy (AFM) and electrochemical impedance spectroscopy (EIS) were employed for the characterization of the biosensor surface at different fabrication steps.

The morphological imaging at the nanoscale after any fabrication steps of the working electrode has been performed by AFM in noncontact mode (NCM). Because this procedure preserves samples by damages, NCM AFM characterization is usually employed to image and measure functionalized nanostructured surfaces, ultrasoft materials, and biological samples, including PNA and DNA sequences.[37]

Figure 4 reports the NCM phase and topography of the working electrode surface during the fabrication process as well as the detection step (Figure 4A–L), including a 3D reconstruction of the working electrode after the gold nanoparticles (AuNPs) deposition and after the last modification step by PNA–miRNA duplex followed by the measurement with $Ru(NH_3)_6^{3+}$ (Figure 4M,N).

The working electrode after AuNPs deposition had an effective surface of about 12 μm^2 (increased with respect to the geometrical scanned surface equal to 9 μm^2) and it appeared in the topography image to be fully covered by AuNPs, the distribution of which was not homogeneous at the micrometric level, indeed AuNPs were aggregated in macro-agglomerates (Figure 4A,B).

After the PNA immobilization (Figure 4C,D), the AuNP aggregates were still clearly visible and completely covered the electrode surface. The NCM phase contrast image did not match the topography contrast, suggesting an inhomogeneous coverage of the AuNPs by PNA. Moreover, a strong increment (from about 12–18 μm^2) of the effective surface of the modified electrode was registered, due to a further ultra-structuration of the exposed AuNPs surfaces.

After 6-mercapto-1-hexanol (MCH) incubation (Figure 4E,F), the effective surface was about the same as the previous fabrication step (17 μm^2) and a similar NCM phase distribution was still present, even if the topography of the macro-aggregates was slightly changed. After miRNA incubation, a further increment in the NCM phase contrast and effective surface (about 22 μm^2) was registered (Figure 4G,H).

Finally, after the $Ru(NH_3)_6^{3+}$ incubation, the NCM phase image and topography were very similar to the sample after the first AuNPs deposition (Figure 4I,L). Moreover, the decreasing of the effective surface suggested a full coverage of the AuNPs by the PNA–miRNA duplex and $Ru(NH_3)_6^{3+}$ interaction.

Successively, EIS characterization was carried out and typical Nyquist plots were obtained before and after drop-casting 8 μL of AuNPs onto the graphite working electrode (**Figure 5**a). AuNPs-modified SPE (purple plot) showed resistance to charge transfer (R_{ct}) equal to 514 ± 21 kΩ, which is lower than the one obtained using bare electrode (black plot), that is, 4325 ± 13 kΩ. This decrease of Rct demonstrated an enhancement of the conductivity after modification with AuNPs, thus AuNPs act both as an anchor for probe immobilization and as nanomaterial to increase the electrochemical performances of the sensor. The R_{ct} increased after PNA immobilization (974 ± 13 kΩ, orange plot) and after incubation with MCH (1474 ± 9 kΩ, cyan plot) is ascribed to the formation of PNA and MCH layers, hindering the reaction at the working electrode surface of the redox couple $[Fe(CN)_6]^{3-/4-}$. After hybridization with the complementary target sequence (green plot), a significant increase of Rct to 3133 ± 13 kΩ was observed due to the negative charge of miRNA-486-5p, resulting in the formation of an electrostatic barrier for the negative $[Fe(CN)_6]^{3-/4-}$.

These EIS results were also confirmed by cyclic voltammetric measurements reported in Figure 5b, which show a typically reversible voltammogram of redox couple $[Fe(CN)_6]^{3-/4-}$. The voltammogram obtained with bare SPE indicated a pair of reversible redox peaks with ΔEp of 0.463 V (Figure 5b, black curve), while after modification by drop-casting of working electrode surface with AuNPs, the intensity of peak currents signal was considerably increased with a decrease of ΔEp, that is,

© 2022 The Authors. Advanced NanoBiomed Research published by Wiley-VCH GmbH

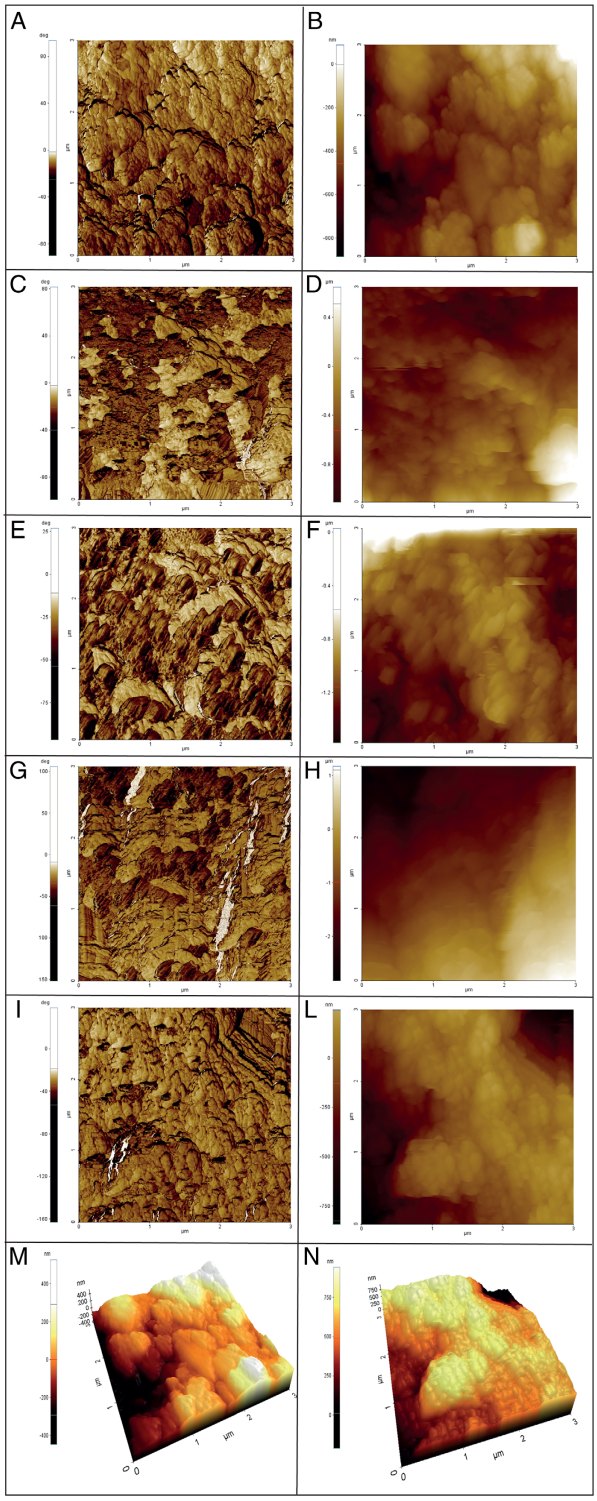

Figure 4. Noncontact mode (NCM) phase and topography images for each step of fabrication and detection of the working electrode: A,B) AuNPs deposition; C,D) PNA incubation; E,F) 6-mercapto-1-hexanol (MCH) incubation; G,H) miRNA incubation; I–L) PNA–miRNA duplex and interaction with $Ru(NH_3)_6^{3+}$. Topographical 3D reconstructions of a $3 \times 3\ \mu m^2$ scanned surfaces of the working electrode after AuNPs deposition (*M*) and after the final modification step by PNA–miRNA duplex and interaction with $Ru(NH_3)_6^{3+}$ (*N*).

0.202 V (Figure 5b, purple curve), confirming that AuNPs provide an improvement in the electrochemical performances of the electrode. The immobilization of PNA probe on AuNPs-modified electrodes cause an increase ΔEp to 0.410 V (Figure 5b, orange curve), and the subsequent incubation with MCH causes a further decrease of the redox peak current with ΔEp = 0.400 V (Figure 5b, cyan curve), due to the cover of the gold sites necessary for electron transfer.[38] At last, SPE was incubated with 100 nM of miRNA-486-5p for 60 min, and the peak currents decreased together with the increase of ΔEp = 0.432 V, due to the electrostatic barrier formation after the hybridization of PNA with the target analyte.

2.4. Optimization of the Experimental Parameters

Before evaluating the biosensor suitability to detect different concentrations of miRNA, we performed the optimization of the experimental parameters that could influence the analytical performances of this sensing tool.

The first parameter optimized was the probe concentration to be immobilized onto the working electrode surface. Four different concentrations were tested, 25, 50, 100, 200 nM, and the results are shown in Figure 5c. 100 nM was the concentration giving the highest signal change and the highest repeatability, given RSD% equal to 8%. Indeed, a decreasing signal was obtained at increasing probe concentration. This probe density dependence of biosensor signaling can result in steric hindrance that could affect the PNA–miRNA interaction.[39]

For this reason, 100 nM was the probe concentration used for miRNA target detection. Moreover, we studied the optimal probe immobilization time for biosensor develpresent in the solutionopment. The times investigated were 30, 60, 120, and 240 min (Figure 5d), and 60 min was selected in terms of repeatability and signal variation obtained (RSD% equal to 8%).

Another critical step was the optimization of the amount of electrochemical mediator to add to the working solution. After the PNA–miRNA duplex formation, the hexaammineruthenium can electrostatically interact with the negatively charged backbone of miRNA and the current signal measured is directly proportional to the amount of $Ru(NH_3)_6^{3+}$ present in the solution.[34] In this study, $Ru(NH_3)_6^{3+}$ concentrations examined were 2.5, 5, and 7.5 mM, 5 mM was chosen, being the lowest amount of mediator used, giving the maximum signal change and lowest RSD%, 6% (Figure 5e). Indeed, a higher amount of redox molecule (10 mM) produced the worst result. Too much redox probe could affect the biosensor response due to the difficulty in removing its excess during the washing steps, resulting in increased background signal at low-miRNA concentrations.

The recognition between PNA and its target miRNA (sequence 5'UCCUGUACUGAGCUGCCCCGAG 3') and the consequent duplex formation are crucial factors to establish the device sensitivity. Moreover, the binding time directly impacts the time of the analysis and its suitability to be used as a non-invasive diagnostic test. Thus, it was necessary to investigate the probe–target interaction, and the binding times tested were 20, 60, 120, and 240 min. Although it is reported in the literature that duplex formation of ≈20 bp requires about 20 min,[40,41] in this work, 60 min were selected as a compromise

© 2022 The Authors. Advanced NanoBiomed Research published by Wiley-VCH GmbH

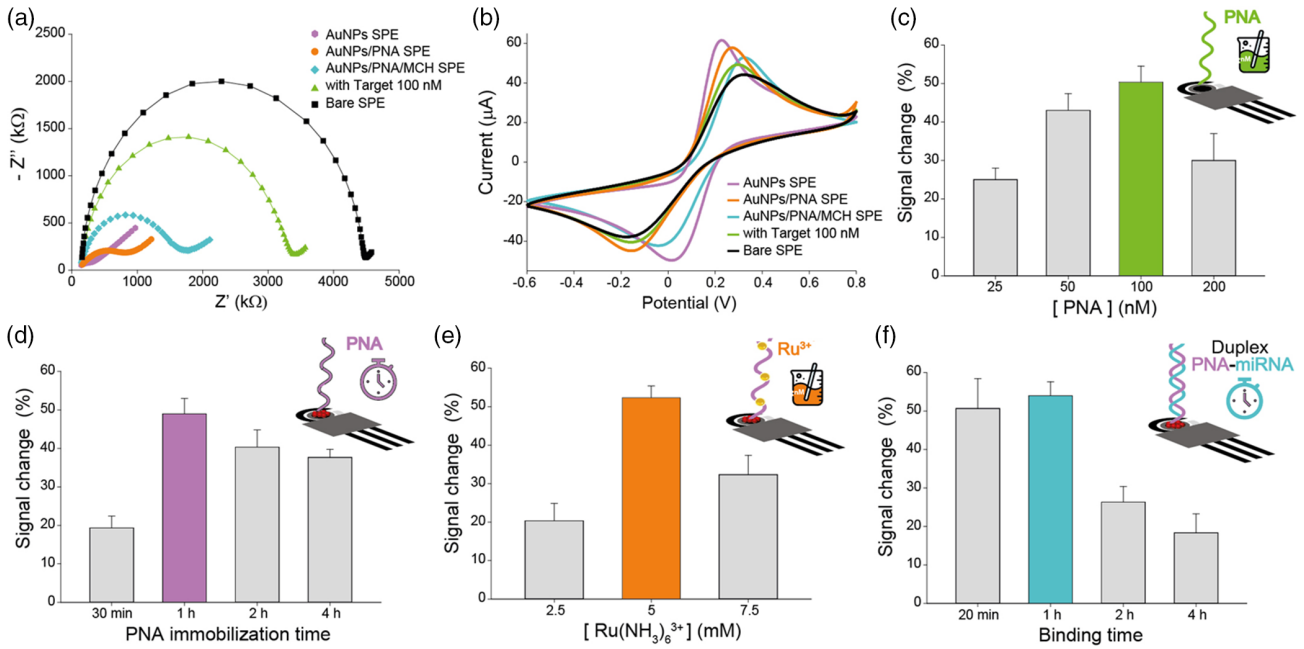

Figure 5. a) Nyquist plots obtained with bare electrode, AuNPs-modified SPE, AuNPs/PNA- (100 nM) modified SPE, AuNPs/PNA (100 nM)/MCH- (2 μM) modified SPE and after PNA (100 nM)-miRNA-486 (100 nM) hybridization. Electrochemical impedance spectroscopy (EIS) measurements were carried out using 100 μL of KCl 0.1 M solution containing $[Fe(CN)_6]^{3-/4-}$ 5 mM was used. b) Voltammograms obtained with bare electrode, AuNPs-modified SPE, AuNPs/PNA- (100 nM) modified SPE, AuNPs/PNA (100 nM)/MCH- (2 μM) modified SPE and after PNA (100 nM)-miRNA-486 (100 nM) hybridization using 100 μL of KCl 0.1 M solution containing $[Fe(CN)_6]^{3-/4-}$ 5 mM was used (potential range from −0.6 to 0.8, scan rate 0.05 V s^{-1}). c) PNA concentration optimization. Concentrations tested: 25, 50, 100, 200 nM in 50 mM phosphate buffer + NaCl 150 mM, pH = 7, in RNase-free water. PNA immobilization time = 60 min. $[Ru(NH_3)_6^{3+}]$ = 5 mM. [miRNA] = 100 nM. Binding time = 20 min. d) PNA immobilization time optimization. Times tested: 30, 60, 120, 240 min. [PNA] = 100 nM. $[Ru(NH_3)_6^{3+}]$ = 5 mM. [miRNA] = 100 nM. Binding time = 20 min. e) $Ru(NH_3)_6^{3+}$ concentration optimization. Concentrations tested: 2.5, 5, 7.5 mM. [PNA] = 100 nM. PNA immobilization time = 60 min. [miRNA] = 100 nM. Binding time = 20 min. f) Binding time optimization. Times tested: 20 min, 1, 2, 4 h. [PNA] = 100 nM. PNA immobilization time = 60 min. $[Ru(NH_3)_6^{3+}]$ = 5 mM. [miRNA] = 100 nM. Measurements were carried out in triplicates (n = 3) for each concentration or condition tested, and the mean ± the error of the three measurements is reported together with relative SD (calculated as SD/mean × 100).

between maximum signal variation and highest repeatability (RSD% equal to 7%); thus, it was chosen as the binding time for further investigations (Figure 5f).

2.5. miRNA-486-5p Detection

Once optimized all the experimental parameters, the device performance was evaluated in the presence of different miRNA-486-5p concentrations using the signal-on approach, which allows for an increase of the measurable signal when the target is present. The concentrations tested ranged between 0.01 nM and 1 μM (prepared in phosphate buffer solution 50 mM containing NaCl 150 mM, pH = 7), and the binding curve obtained is shown in **Figure 6**a. The curve was fitted to the hyperbolic Langmuir isotherm with $R^2 = 0.976$ and an affinity constant equal to 28 ± 4 nM. Moreover, a linear range between 10 and 100 nM was obtained with a calculated limit of detection of 0.5 nM, which corresponds to the amount of target able to produce a current signal equal to 3 times the deviation standard of the blank.

After evaluating the analytical performance of the biosensor in standard solution, the device was tested in serum samples kindly provided by healthy volunteers. In detail, undiluted serum was spiked with different concentrations of miRNA-486-5p (from 0.01 nM to 1 μM), giving the binding curve fitted by using hyperbolic Langmuir isotherm ($R^2 = 0.972$). Figure 6b shows a linearity from 10 to 100 nM with an affinity constant of 28 ± 7 nM and the limit of detection equal to 0.7 nM.

The reproducibility was assessed by measuring each concentration of the calibration curve in triplicate with RSD% values lower than 10%, for instance, RSD% = 7% for 10 nM, RSD% = 5% for 50 nM, and RSD% = 4% for 100 nM. These results showed the suitability of the printed biosensor to detect different concentrations of miRNA target with high sensitivity and reproducibility, even in a complex matrix such as serum. Furthermore, this sensor demonstrated valuable analytical features when compared with the other sensing tools reported in the literature (Table S1, Supporting Information).

2.6. Selectivity and Storage Stability Studies

The selectivity of the biosensor was investigated by measuring sequences differing from the target sequence, even for a single base. The sequences tested were the following: 1 mismatched at 3' end of the oligonucleotide sequence, 1MM 3' (5'

© 2022 The Authors. Advanced NanoBiomed Research published by Wiley-VCH GmbH

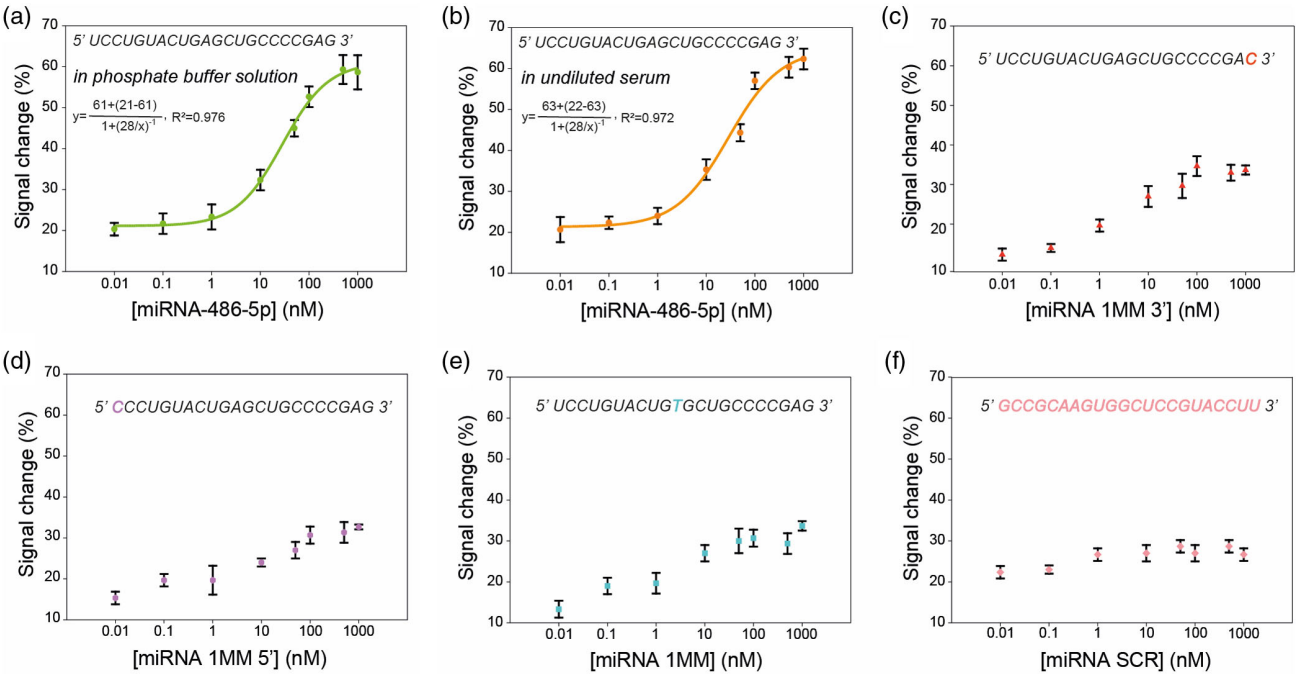

Figure 6. a) Binding curve in standard solution. Concentrations tested comprised in the range between 0.01 nM and 1 μM in 50 mM phosphate buffer + NaCl 150 mM, pH = 7, in RNase-free water. [PNA] = 100 nM. PNA immobilization time = 60 min. $[Ru(NH_3)_6^{3+}]$ = 5 mM. Binding time = 60 min. b) Binding curve in undiluted serum sample. Concentrations tested comprised in the range between 0.01 nM and 1 μM in undiluted serum sample. [PNA] = 100 nM. PNA immobilization time = 60 min. $[Ru(NH_3)_6^{3+}]$ = 5 mM. Binding time = 60 min. c) Calibration curve of 1MM 3', d) calibration curve of 1MM 5', e) calibration curve of 1MM, and f) calibration curve of RNA scrambled obtained testing different concentrations in the range comprised between 0.01 and 1000 nM in serum samples. Experimental condition: [PNA] = 100 nM, PNA immobilization time = 60 min, $[Ru(NH_3)_6^{3+}]$ = 5 mM and binding time = 60 min. Measurements were carried out in triplicates ($n = 3$) for each concentration or condition tested, and the mean ± the error of the three measurements is reported together with relative SD (calculated as SD/mean × 100).

UCCUGUACUGAGCUGCCCCGAC 3'); 1 mismatched at 5' end, 1MM 5' (5'CCCUGUACUGAGCUGCCCCGAG 3'); 1 mismatched at the central zone of the sequence, 1MM (5'UCCUGUACUGTGCUGCCCCGAG 3') and a fully random sequence, scrambled (SCR)–RNA (5' GCCGCAAGUGG CUCCGUACCUU 3'). The calibration curves of these sequences were compared with the calibration curve of miRNA-486 obtained in the same experimental conditions (serum sample and concentration tested in the range comprised between 0.01 and 1000 nM). The results are shown in Figure 6. All the non-complementary sequences, 1MM 3' (Figure. 6c), 1MM 5' (Figure 6d), 1MM (Figure 6e), and SCR–RNA (Figure 6f), caused no proper signal variations even at higher concentration with respect to miRNA-486-5p, demonstrating the excellent selectivity of the biosensor developed toward the target analyte even in the case of single mismatches.

Furthermore, the storage stability of the electrochemical biosensor was evaluated at RT temperature, and the results are reported in Figure S1, Supporting Information. The miRNA-486-5p was measured after 1, 2, 3 d and 1, 2, 3, and 4 weeks after the biosensor fabrication. Figure S2, Supporting Information, shows that after 1 day we obtained a decrease in the signal change equal to 5%, after 2 weeks a decrease of 10% and after the third week, the electrochemical biosensor resulted stable with a decrease of the electrochemical signal change of the 40%.

2.7. Detection of miRNA-486–5p Expression on Serum by Electrochemical Platform

To evaluate if the device was able to detect miRNA-486-5p also in real matrix, the electrochemical platform was used to detect the miRNA target in the serum samples of the 12 CD patients before and after one year of a GFD, the 14 IBS patients and the 14 healthy volunteers. In conformity with the results provided by RT-qPCR, the miRNA-486-5p expression was 2.2 ± 0.4 times higher in CD patients with respect to healthy cases and 1.7 ± 0.3 and 1.8 ± 0.3 times higher with respect to GFD patients and IBS patients, respectively (**Figure 7**). With these results, the device showed suitability to measure the miRNA target also in serum sample of CD patients before and after GFD giving good results in monitoring the treatment.

3. Conclusions

Herein, we identified a novel biomarker in serum namely miRNA-486-5p for the no-invasive diagnosis of CD, by analyzing the serum of the cohorts of recruited subjects by the qRT-PCR technique. For the design of a smart analytical tool for miRNA-486-5p detection, printed electrochemical chip has been fabricated and modified with AuNPs and PNA probe to deliver an easy to use the device, able to work in standard solution and the

© 2022 The Authors. Advanced NanoBiomed Research published by Wiley-VCH GmbH

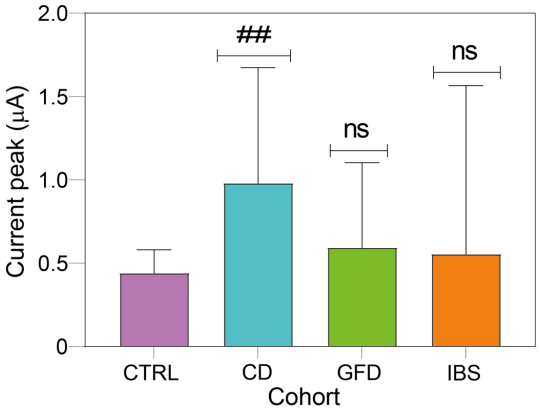

Figure 7. miRNA-486-5p expression in four cohorts: control, coeliac disease patients, patients under gluten-free diet, and patients with irritable bowel syndrome detected by electrochemical platform. [PNA] = 100 nM. PNA immobilization time = 60 min. $[Ru(NH_3)_6^{3+}] = 5$ mM. Binding time = 60 min. Data are shown as multiple unpaired *t*-test. $^{\#\#}p < 0.01$.

untreated serum sample, with a limit of detection equal to 0.5 and 0.7 nM, respectively.

The results obtained by testing serum samples from 12 CD patients before and after 1 year of a GFD, 14 IBS patients, and 14 healthy volunteers demonstrated the suitability of the developed miniaturized device for diagnosis and prognosis of CD, paving the way for the application of electrochemical miniaturized PNA-based biosensor in autoimmune pathologies.

The novelty of this work relies on the identification of a useful biomarker in serum for CD and the development of novel smartphone-assisted electrochemical chip for the selected biomarker detection in serum, enlarging the use of the electrochemical printed biosensor beyond the glucose strip and boosting furtherly the use of point-of-care devices for smart management of diseases.

4. Experimental Section

Reagents and Equipment: Sodium chloride, sodium dihydrogen phosphate hydrate (NaH_2PO_4 H_2O), sodium hydrogen phosphate (Na_2HPO_4), MCH, and tris(2-carboxyethyl)phosphine hydrochloride (TCEP), hexaamminerutheniumIII) chloride ($Ru(NH_3)_6Cl_3$) were purchased from Sigma-Aldrich (St. Louis, MO, USA). AuNPs (5 nm diameter) were synthesized following the procedure described in our previous work.[36] Polyester-based screen-printed electrodes were supplied from Sense4Med Company (Rome, Italy), composed of graphite counter and working electrodes and silver/silver chloride pseudoreference electrodes. All the electrochemical measurements were carried out using a miniaturized potentiostat Sensit Smart (PalmSens, Netherlands) connected to a smartphone. The EIS was performed in $[Fe(CN)_6]^{3-/4-}$ (5 mM) + KCl (0.1 M), and the resistance to charge transfer was calculated using Randles circuit and Z-View software.

miRNA-486-5p was purchased from ChemGenes Corp., Wilmington, Massachusetts, USA while the RNA sequences for the selectivity study were purchased from Biomers.net the polymer factory Ulm (Germany). For the synthesis of PNA, the Fmoc-PAL-polyethylene glycol (PEG)-polystyrene (PS) resin was used, supplied by Applied Biosystem. The hydroxybenzotriazole (HOBT) activators, hexafluorophosphate benzotriazole tetramethyl uronium (HBTU) were purchased from Novabiochem, 2-(1H-7-Azabenzotriazol-1-yl)-1,1,3,3-tetramethyluronoium hexafluorophosphate (HATU) was purchased from IRIS Biotech GMBH, while piperidine, N,N-diisopropylethylamine (DIPEA), acetic anhydride, and TFA were supplied by Biosolve, the N, methyl-morpholine (NMM) was provided by the company Sigma-Aldrich. The anhydrous solvents for the synthesis of PNAs (DCM, DMF) were supplied by the company J.T.Baker. Fmoc-PNA-cytosine(Bhoc)-OH, Fmoc-PNA-thymine-OH, Fmoc-PNA-guanine(Bhoc)-OH, and Fmoc-PNA-adenine(Bhoc)-OH were provided by Link Technologies. Fmoc-Ahx-OH was supplied by Sigma-Aldrich, while Fmoc-Cys (trt) -OH from Iris Biochem. The analyses and purification of the products were carried out by high-pressure reverse-phase liquid chromatography (RP-HPLC). Analytical analyzes and purification of PNA oligomers were performed on Agilent 1100 (Hewlett Packard) analytical HPLC equipped with a UV detector and autosampler. A Phenomenex Jupiter (5 μm C18 300 Å, 4.6 × 250 mm) column was used at a flow of 1 mL min^{-1}. Liquid chromatography-mass spectrometry (LC-MS) analyses were conducted using a Phenomenex Jupiter (5 μm C18 300 Å column, 150 × 460 nm), on an instrument from a Surveyor series HPLC, coupled to a Thermo Finnigan mass spectrometer equipped with an electrospray source and a time of flight analyzer.

RNA Extraction: To carry out a gene expression analysis using the RT-PCR technique, it is necessary to isolate the RNA. The validity and precision of gene expression estimated by RT-PCR were totally influenced by the quality, purity, and integrity of the starting genetic material. To be considered as "high quality" RNA to be used in the retro-transcription, it must be free of RNase, proteins, and genomic DNA.[42,43]

Due to the greater abundance of RNA in cells than in body fluids, even small amounts of cell debris may significantly affect RNA profiling of cell-free fluids such as serum. Therefore, high g-force centrifugation was performed to isolate circulating nucleic acids from serum samples to remove all cell debris potentially present in them. This centrifugation step significantly reduces the amount of cellular or genomic DNA and cellular RNA in the samples.

In particular, the serum samples (approximately 1 mL) were centrifuged in Eppendorf (10 min, 16 000 g) in a refrigerated centrifuge with a fixed-angle rotor, and the obtained supernatant was carefully transferred to a new tube that does not damage the pellet. The samples were subsequently aliquoted and frozen at −80 °C.

Among the specific kits for the extraction of small RNA commercially available, two were selected: the MagMAX mirVana (Applied Biosystems) and the miRNeasy Serum/Plasma Kit (Qiagen).

MagMAX mirVana enabled the isolation of total RNA, including miRNAs, from a wide variety of matrices, including serum and plasma. The kit used magnetic beads, which ensure a high yield of high-quality RNA. The extraction protocol included several steps: initial digestion of the serum samples performed with proteinase K, the addition of the lysing agent 2-mercaptoethanol, followed by the addition of the magnetic beads that bind RNA, and by several washes with appropriate solutions and isopropanol. The samples were treated with DNase, and after proper washing and subsequent binding with the beads, we proceed with the final elution of the RNA in a specific elution buffer.

The miRNeasy Serum/Plasma Kit (Qiagen) was specifically designed to purify total RNA, including miRNAs, from animal and human plasma and serum. It used a phenol/guanidine solution for the lysis of samples, followed by the purification of total RNA through a silica membrane. QIAzol Lysis Reagent was a monophasic solution of phenol and guanidine thiocyanate that facilitated the lysing process, denatured protein complexes and RNases, and removed most of the DNA with residual proteins from the lysate by organic extraction. First, QIAzol was added to serum samples. After the addition of chloroform, the lysate was separated into the aqueous and organic phases by centrifugation. RNA migrated in the upper aqueous phase, DNA at the interphase, and proteins in the lower organic phase and interphase. Then, the upper aqueous phase was separated, and ethanol was added to provide appropriate binding conditions for all RNA molecules, approximately 18 nucleotides long. The sample was then placed into the RNeasy MinElute spin column, where the total RNA would bind to the membrane while the phenol and other contaminants were washed away. The RNA was then eluted in a small volume of RNase-free water.

© 2022 The Authors. Advanced NanoBiomed Research published by Wiley-VCH GmbH

Both techniques were tried, and the miRNeasy Serum/Plasma Kit was selected for the RNA extractions due to its easier applicability.

To identify the expression profile of miRNAs in serum or plasma samples, there was currently no shared opinion within the scientific community regarding the use of normalizers. The most common trend is to insert a synthetic miRNA (Spike-In) into samples to monitor the quality of RNA extraction and cDNA synthesis. The Spike-In was inserted into the samples after adding the denaturant (e.g., QIAzol), followed by adding the chloroform and subsequent separation phase.

The use of the Spike-In Control was strongly recommended to evaluate the purification and amplification of miRNAs. Indeed, the yield of RNA extracted from serum or plasma was highly variable from sample to sample coming from different individuals and was generally too low for quantification by measuring its optical density (e.g., Nanodrop). The use of a normalizer allowed overcoming this limit since, after RT-PCR, the obtained cycle threshold (CT) value relative to the synthetic miRNA allowed the normalization between the different samples.

Cel-miR-39-3p (Thermo Fisher Scientific) extracted from *Caenorhabditis elegans* has been selected among the recommended Spike-In, whose nucleotide sequence is shown as follows:

cel-miRNA-39-3p: 5' UCACCGGGUGUAAAUCAGCUUG 3'

The lyophilized preparation of cell-miRNA-39-3p was first resuspended in RNase-free water to obtain a solution with a concentration of 100 μM; subsequently, dilutions were carried out until a concentration of 10 μM was reached. Aliquots of the obtained solution were stored at −80 °C.

Extraction protocol: 1) Serum samples stored at −80 °C were thawed and brought to room temperature (15–25 °C); 2) 100 μL of serum was collected for each sample to which 5 volumes (500 μL) of QIAzol Lysis Reagent were added; 3) tubes containing lysate were vortexed and left at room temperature for 5 min; 4) to each sample, Spike-In Control (3.5 μL, 10 pM) (cel-miR-39-3p) was added and the solutions thoroughly mixed; 5) chloroform (100 μL) was added to the matrix and vortexed (15 s) until a completely homogeneous solution was obtained; 6) after incubation (2–3 min) at room temperature, the tubes were centrifuged (12 000 g, for 15 min, 4 °C). Separation of three phases was obtained: an upper aqueous phase, colorless, containing RNA; white interphase containing DNA; and a red lower organic phase containing proteins and lipids; 7) the upper phase (approximately 300 μL) was transferred to a new tube, and 1.5 volumes (450 μL) of 100% ethanol were added by mixing thoroughly; 8) 700 μL of each sample were pipetted into a RNeasy MinElute spin column and centrifuged (8000 g, 15 s, 15–25 °C); the contents of the collection tube were discarded; 9) the membranes were washed with suitable buffers by centrifuging (15 s, 8000 g), and a final wash was carried out with 80% ethanol (8000 g for 2 min); 10) the RNeasy MinElute spin columns, with an open lid, were centrifuged at maximum speed for 5 min to dry the membranes well. This step is crucial to eliminate any ethanol residues that could interfere with subsequent reactions; 11) to each column, RNase-free water (14 μL) was added directly to the center of the membrane, and centrifugation (1 min) was carried out at maximum speed to elute RNA; and 12) The RNA obtained was stored at −80 °C.

Analysis of MicroRNA Expression by using RT-PCR: RT-PCR, or qPCR (quantitative PCR), allowed to quantify the PCR product's synthesis at each amplification cycle in real-time. This technique allowed a quantitative analysis of the amount of initial DNA template (or cDNA), and that is why RT-PCR is often used, in combination with the retro-transcription reaction (RT), to quantify the levels of expression of specific genes. The signal was quantified by the fluorescence emitted by fluorophores (fluorescent dyes) to bind the DNA molecules produced at each amplification cycle. The fluorophores could intercalate with DNA in a nonspecific way or act as markers of oligonucleotide probes complementary to specific sequences. In our experiments, the TaqMan probe, a hydrolytic probe with a high-energy fluorophore (reporter) at the 5' untranslated region (UTR), and a fluorophore inhibitor (quencher) at the 3' UTR, was used. When the probe was paired with the target sequence, the inhibitor was close enough to the fluorophore to block the emission of the fluorescent signal. During the elongation, in each amplification cycle, the polymerase hydrolyzed the probe. In this way, the fluorophore was released into the reaction mixture and moved away from the inhibitor, resulting in the emission of the fluorescent signal. The emission of the fluorescent signal depends on the activity of the Taq DNA polymerase.

During the PCR cycles, the collection of the fluorescent signal took place, and the intensity of the fluorescence of the reaction mixture in each well was measured and plotted with respect to the reaction cycle. If a target is present, its amplification can be monitored in real time.

For the expression analysis of the miRNAs of our interest, the TaqMan Advanced miRNA cDNA Synthesis Kit and the TaqMan Advanced miRNA Assays (Applied Biosystems) were used.

The TaqMan Advanced miRNA cDNA Synthesis Kit allowed the preparation of cDNA templates from the entire pool of mature microRNAs present in the sample.

miRNAs were modified by ligation of an adapter at the 5' UTR and extension of the 3' UTR of the mature transcript by adding a poly(A) tail. Modified miRNAs underwent a reverse transcription reaction followed by a miRNA cDNA amplification reaction (miR-Amp).

Following assays (TaqMan Advanced miRNA Assays) were characterized by specific probes and primers for a specific target and could detect and quantify the expression levels of the miRNAs of interest through qPCR analysis. The assays can detect mature forms of miRNAs starting from 2 μL of total RNA from serum or plasma.

When working out with small RNA, any slight variations in the quantity of starting material, the modalities of sample collection, the purification and quality of the RNA, and the efficiency of the reverse transcription can determine errors in quantifying the expression level.

Normalization with an endogenous constitutively expressed control gene is currently the most accurate method for correcting potential bias. An ideal endogenous control shows a relatively constant and moderately abundant expression level in various tissues and cell types and various types of treatment.

In our experiments, miRNA-16-5p was selected because it was reported in the literature and known to be expressed at relatively constant levels in plasma and serum:

miRNA-16-5p 5' UAGCAGCACGUAAAUAUUGGCG 3'

Nevertheless, it is always suggested to validate the chosen endogenous control, or a set of controls, since no control can act as a universal endogenous control under all experimental conditions.[44]

Protocol: 1) Polyadenylation: 2 μL of RNA from each sample were treated with a mix of Poly(A) Buffer, ATP, Poly(A) Enzyme, and RNase-free water and loaded into the thermal cycler for the polyadenylation reaction at the 3' UTR (37 °C 45 min, 65 °C 10 min, 4 °C storage); 2) Ligation: after having prepared a reaction mix with appropriate volumes of 50% polyethylene glycol (PEG) 8000, Ligation Adapter, DNA Ligase Buffer, RNA Ligase, and RNase-free water, 10 μL of this mix were added to 5 μL of the product of previously obtained polyadenylation and the ligation reaction was carried out in a thermal cycler (16 °C, 60 min, 4 °C storage); 3) Retrotranscription: 15 μL of the product obtained from the ligation reaction were treated with 15 μL of a mix composed of dNTP, Universal RT primer, RT Enzyme Mix, RT Buffer, and RNase water followed by the reverse transcription reaction (42 °C, 15 min, 85 °C 5 min, 4 °C storage); 4) miR-Amplification: a mix containing miR-Amp Master Mix, miR-Amp Primer Mix, and RNase-free water were prepared, and 45 μL of this mix was added to 5 μL of the previously obtained product and was performed at thermal cycler the specific amplification reaction for miRNAs: a) activation of the enzyme: at 95 °C 5 min; b) denaturation: at 95 °C 3 s for 14 cycles; c) annealing and extension: at 60 °C, 30 s for 14 cycles; d) stop reaction: at 99 °C, 10 min; and e) storage: at 4 °C; 5) RT-PCR: a 1:10 dilution of products obtained from the miR-Amplification with TE buffer was carried out, the Fast Advanced Master mix (15 μL) was added to this diluted cDNA (5 μL), and TaqMan Advanced miRNA Assays were specific to the targets of interest. The 52 samples to be analyzed were aliquoted for the different assays and loaded on the 96-well reaction plates, already containing the targets of interest (miRNA-449, miRNA-492, miRNA-21-5p, and miRNA-486-5p), the endogenous control (miRNA-16-5p), and the exogenous control (cel-miR-39-3p). A healthy subject was chosen to be used as a calibrator, loaded on each plate, and used as a reference for comparative analysis. A technical replicate was performed for each sample to improve accuracy and exclude operator errors

© 2022 The Authors. Advanced NanoBiomed Research published by Wiley-VCH GmbH

in the dispensing phase of samples. Negative controls necessary to identify the presence of nonspecific products or sample contamination were included in each assay. The negative control consists of all components of the reaction mixture except the genetic material to be amplified.

The qPCR analysis was performed on the StepOnePlus Real-Time PCR System instrument (Thermo Fisher Scientific) in compliance with the following protocol: 1) activation of the enzyme: at 95 °C, 20 s; 2) denaturation: at 95 °C, 3 s for 40 cycles; and 3) annealing and extension: at 60 °, 30 s for 40 cycles.

Data Analysis: RT-PCR signal analysis was performed with the software StepOne and StepOnePlus Software v2.3. For the analysis of miRNA expression levels, relative quantification of the fluorescence signal was performed. The Cycle threshold (Ct) of each sample is inversely proportional to the initial quantity; this means that the smallest is the quantity of starting material, more cycles will be required to reach the threshold level. With a relative quantification, it is possible to determine the changes in the expression levels of a target miRNA in different samples compared to internal control, which can be co-amplified together with the target of interest. The endogenous control is a reference miRNA whose expression level remains constant in all tested samples and is not affected by experimental treatments. A reference control is advantageous, especially when quantifying the starting material is impossible or when a small amount of initial template is available.

For each experiment, the following agents are needed: 1) target: the cDNA sequence to be analyzed; 2) calibrator: the sample to be used as a reference for comparative analysis; and 3) endogenous control: an miRNA constitutively expressed in all samples, necessary to normalize the data with respect to the quantity of loaded cDNA and any variations in the efficiency of the reaction.

The calibrator was used when comparing multiple samples; the expression of the target miRNAs in all samples was represented by a relative increase or decrease compared to the calibrator. The advantage of the method based on the normalizer with reference genes or miRNAs was represented by chance to avoid an absolute quantification and the need to have an exact quantification of the template loaded for the reaction.

The relative quantification of miRNA expression was performed with the $2^{(-\Delta\Delta Ct)}$ method. It assumed the hypothesis that both target and reference genes were amplified with an efficiency of approximately 100%, with an acceptable deviation of 5%. Therefore, it is necessary to verify the validity of this hypothesis, checking the amplification efficiencies of both the target genes and the reference genes. Once established that the initial hypothesis is correct, it was possible to proceed with the normalization of target gene (or miRNA) Ct with respect to the reference gene (or miRNA, ref), both for treated samples (test) and for controls (cal).

$$\Delta Ct\,(test) = Ct\,(target,\ test) - Ct\,(ref,\ test) \tag{1}$$

$$\Delta Ct\,(cal) = Ct\,(target,\ cal) - Ct\,(ref,\ cal) \tag{2}$$

ΔCT of the test must be normalized with the ΔCt of the calibrator

$$\Delta\Delta Ct = \Delta Ct\,(test) - \Delta Ct\,(cal) \tag{3}$$

$$Ratio = 2^{-\Delta\Delta Ct} \tag{4}$$

In our case, the reference miRNA (ref) was represented by the miRNA-16-5p, while the control sample (cal) was the healthy (non-coeliac) subject chosen[45] as a reference and reported in each assay. The result obtained quantified the increase (or decrease) of the target gene in the test sample relative to the calibrator sample and normalized with respect to the expression of the reference gene.[44]

Assuming a value of $\Delta\Delta CT > 0$, which corresponded to the condition in which ΔCT (test) > ΔCT (cal), and substituting its value in the expression of the ratio, we obtained a ratio < 1, index of under-expression of the gene of interest in the sample treated (test), compared to the control sample (cal). Conversely, a value of $\Delta\Delta CT > 0$, that is, ΔCT (test) < ΔCT (cal), gave a ratio > 1, which corresponded to an increase in gene expression in the treated sample compared to the control.

PNA Bioprobe Synthesis: PNA bioprobe was synthesized employing a synthetic protocol still reported in literature which consisted of repetitive cycles of deprotection, coupling and acetylation, at room temperature.[46] To improve the efficiency of the coupling reaction, double couplings were performed on G and A monomers. The Cys conjugate was obtained adding Fmoc-Ahx-OH and Fmoc-Cys (trt)-OH at the N terminus of PNA oligomer still immobilized on resin and employing the standard synthetic procedure for peptide synthesis. The purification of PNA was carried out through RP-HPLC on a semi-preparative column, using a gradient of acetonitrile (0.1% TFA) in H_2O (0.1% TFA) from 5% to 70% in 30 min. The purified product was characterized by electrospray ionization time-of-flight (ESI-TOF) mass spectrometry.

Cys-Ahx-AntimiR-486-5p: Cys-Ahx-ctcggggcagctcagtacagga (Da): found: 6243.6600; $[M+3H]^{3+}$: 2082.1577; $[M+4H]^{4+}$: 1561.9401; $[M+5H]^{5+}$: 1249.8037; calculated: 6243.1016; $[M+3H]^{3+}$: 2082.0339; $[M+4H]^{4+}$: 1561.7754; $[M+5H]^{5+}$: 1249.6203;

Electrochemical PNA-Based Chip Preparation: First, for the immobilization of PNA oligomer, AuNPs (8 µL) were previously drop-cast onto the working electrode surface to anchor the PNA sequence thanks to the thiol group introduced at the N terminus of the oligomer. The modification with AuNPs and relative working area were evaluated using cyclic voltammetry as technique in 0.1 M H_2SO_4.[47] Then, PNA (100 µM) prepared in phosphate buffer (50 mM) containing NaCl (150 mM) (pH = 7, in RNase-free water) was reduced for 1 h in the presence of TCEP (10 mM), prepared in phosphate buffer (50 mM) containing NaCl (150 mM) (pH = 7, in RNase-free water). After the reduction, the PNA (20 µL of 100 nM) was immobilized onto the SPE surface for 1 h at room temperature in a humid chamber. Successively, the screen-printed electrodes were rinsed with RNase-free water to remove the excess PNA, and they were incubated with 6-mercapto-1-hexanol (20 µL of 2 mM) prepared in phosphate buffer (50 mM) + NaCl (150 mM) (pH = 7, in RNase-free water) to passivate the electrode surface to help PNA-miRNA duplex formation. Then, SPEs were rinsed again with RNase-free water to wash away the unbound MCH, and they were stored with a buffer solution at 4 °C in a humid chamber.

Electrochemical Analysis: In detail, all the electrochemical measurements were performed by differential pulse voltammetry technique (DPV) scanning the potential from −0.1 to −0.5 V using as a working solution 50 mM phosphate buffer containing NaCl 150 mM prepared in RNase-free water at pH 7. The detection of miRNA-486-5p was carried out by comparing the signal obtained in the absence of the target (blank signal) with the signal recorded in the presence of the miRNA-486-5p. For the blank signal, 5 µL of the redox mediator (final concentration 5 mM) were added to the working solution on the PNA-modified SPE. After 20 min, the SPE was rinsed with RNase-free water to wash away the mediator in excess, and the voltammetric measurement was carried out in a buffer solution. Although the PNA was uncharged, a slight peak was observed due to nonspecific interactions between probe and mediator (Figure 1b). The PNA-modified SPE was then incubated with the desired concentration of miRNA-486-5p for 60 min. After the duplex formation, 5 µL of $Ru(NH_3)_6^{3+}$ (final concentration 5 mM) were added to the solution, and after 20 min, the SPE was rinsed with RNase-free water to remove all the unbound molecules. Finally, 100 µL of buffer solution was added to the SPE surface, and the square-wave voltammetry (SWV) scanning was performed. In this case, an increase of the signal is obtained thanks to the electrostatic interactions between the positively charged $Ru(NH_3)_6^{3+}$ and the negative charges of miRNA-486-5p (Figure 1c). The presence of the target was quantified in comparison with the signal recorded in the absence of the target and the signal change obtained was plotted against the concentration of miRNA analyzed. For the detection of miRNA-486-5p, a miniaturized electrochemical chip connected to a smartphone-assisted portable potentiostat was used.

Statics: For microRNA analysis in RT-PCR, each sample of serum was tested in triplicate ($n = 3$) and data expressed as mean ± SD from at least 3 independent experiments ($n \geq 3$). Analysis was performed using one-way analysis of variance (one-way ANOVA) with unpaired *t*-test. $p < 0.05$ was considered to be statistically significant, $p < 0.05$ in

© 2022 The Authors. Advanced NanoBiomed Research published by Wiley-VCH GmbH

comparison with control group, and $*p < 0.1$, $**p < 0.01$, $***p < 0.001$ pathological group. The software used was GraphPad 3.0.

Supporting Information

Supporting Information is available from the Wiley Online Library or from the author.

Acknowledgements

V.C. and M.M. contributed equally to this work. M.M., M.S., and N.A.C. acknowledged H2020-PON-MISE 2014/2020—Project. n. F/050013/03/X32. D.M. acknowledges PRIN 2017 prot. 2017Y2PAB8_004 project "Cutting Edge Analytical Chemistry Methodologies and Bio-Tools to Boost Precision Medicine in Hormone-Related Diseases."

Conflict of Interest

The authors declare no conflict of interest.

Data Availability Statement

The data that support the findings of this study are available from the corresponding author upon reasonable request.

Keywords

PNA, point-of-care devices, screen-printed electrodes, smartphone-assisted potentiostat

Received: February 21, 2022
Revised: May 13, 2022
Published online:

[1] F. Biagi, G. R. Corazza, *Nat. Rev. Gastroenterol. Hepatol.* **2010**, *7*, 158.
[2] P. H. R. Green, C. Cellier, *N. Engl. J. Med.* **2007**, *357*, 1731.
[3] N. Chand, A. A. Mihas, *J. Clin. Gastroenterol.* **2006**, *40*, 3.
[4] P. H. Green, B. Jabri, *Lancet* **2003**, *362*, 383.
[5] A. Fasano, C. Catassi, *N. Engl. J. Med.* **2012**, *367*, 2419.
[6] P. Singh, S. Arora, A. Singh, T. A. Strand, G. K. Makharia, *J. Gastroenterol. Hepatol.* **2016**, *31*, 1095.
[7] S. Ashtari, M. A. Pourhoseingholi, K. Rostami, M. Rostami-Nejad, L. Busani, M. R. Tavirani, M. R. Zali, *JGLD* **2019**, *28*, 95.
[8] R. Costa Gomes, J. Cerqueira Maia, R. Fernando Arrais, C. André Nunes Jatobá, M. Auxiliadora Carvalho Rocha, M. Edinilma Felinto Brito, A. Laissa Oliveira Nazion, C. Marques Maranhão, H. De Sousa Maranhão, *Scand. J. Gastroenterol.* **2016**, *51*, 178.
[9] U. Volta, A. Fabbri, C. Parisi, M. Piscaglia, G. Caio, F. Tovoli, E. Fiorini, *Expert Rev. Gastroenterol. Hepatol.* **2010**, *4*, 31.
[10] W. P. Pais, D. R. Duerksen, N. M. Pettigrew, C. N. Bernstein, *Gastrointest. Endosc.* **2008**, *67*, 1082.
[11] World Economic Forum, Top 10 Emerging Technologies 2017, http://www3.weforum.org/docs/WEF_Top_10_Emerging_Technologies_report_2017.pdf (accessed: September 2021).
[12] M. Capuano, L. Iaffaldano, N. Tinto, D. Montanaro, V. Capobianco, V. Izzo, F. Tucci, G. Troncone, L. Greco, L. Sacchetti, *PLoS One* **2011**, *6*, e29094.
[13] V. Vaira, L. Roncoroni, D. Barisani, G. Gaudioso, S. Bosari, G. Bulfamante, L. Doneda, D. Conte, C. Tomba, M. T. Bardella, S. Ferrero, M. Locatelli, L. Elli, *Clin. Sci.* **2014**, *126*, 417.
[14] S. Magni, G. B. Comani, L. Elli, S. Vanessi, E. Ballarini, G. Nicolini, M. Rusconi, M. Castoldi, R. Meneveri, M. U. Muckenthaler, M. T. Bardella, D. Barisani, *Am. J. Gastroenterol.* **2014**, *109*, 1662.
[15] A. Baldassarre, C. Felli, G. Prantera, A. Masotti, *Genes* **2017**, *8*, 234.
[16] Y. Cai, X. Yu, S. Hu, J. Yu, *Genomics, Proteomics Bioinf.* **2009**, *7*, 102.
[17] W. Filipowicz, S. N. Bhattacharyya, N. Sonenberg, *Nat. Rev. Genet.* **2008**, *9*, 102.
[18] K. A. Bascuñán, F. Pérez-Bravo, G. Gaudioso, V. Vaira, L. Roncoroni, L. Elli, E. Monguzzi, M. Araya, *Dig. Dis. Sci.* **2020**, *65*, 1982.
[19] M. K. Masud, M. Umer, M. S. A. Hossain, Y. Yamauchi, N. T. Nguyen, M. J. Shiddiky, *Trends Biochem. Sci.* **2019**, *44*, 433.
[20] Y. Wang, Z. Li, Q. Lin, Y. Wei, J. Wang, Y. Li, R. Yang, Q. Yuan, *ACS Sensors* **2019**, *4*, 2124.
[21] J. K. Cheong, Y. C. Tang, L. Zhou, H. Cheng, H. P. Too, *Curr. Opin. Biotechnol.* **2022**, *74*, 2124.
[22] M. N. Islam, M. K. Masud, M. H. Haque, M. S. A. Hossain, Y. Yamauchi, N. T. Nguyen, M. J. Shiddiky, *Small Methods* **2017**, *1*, 1700131.
[23] R. Tavallaie, J. McCarroll, M. Le Grand, N. Ariotti, W. Schuhmann, E. Bakker, R. D. Tilley, D. B. Hibbert, M. Kavallaris, J. J. Gooding, *Nat. Nanotech.* **2018**, *13*, 1066.
[24] J. Guo, R. Shen, X. Shen, B. Zeng, N. Yang, H. Liang, Y. Yang, Q. Yuan, *Chin. Chem. Lett.* **2022**, *33*, 979.
[25] M. Umer, N. B. Aziz, R. G. Mahmudunnabi, Y. B. Shim, C. Salomon, M. J. Shiddiky, *Analyst* **2021**, *146*, 5496.
[26] M. N. Islam, M. K. Masud, N. T. Nguyen, V. Gopalan, H. R. Alamri, Z. Alothman, M. S. Al Hossain, Y. Yamauchi, A. K. Lamd, M. J. Shiddiky, *Biosens. Bioelectron.* **2018**, *101*, 275.
[27] M. N. Islam, V. Gopalan, M. H. Haque, M. K. Masud, M. S. Al Hossain, Y. Yamauchi, N. Nguyen, A. K. Lam, M. J. Shiddiky, *Biosens. Bioelectron.* **2017**, *98*, 227.
[28] S. Shin Low, Y. Pan, D. Ji, Y. Li, Y. Lu, Y. He, Q. Chen, Q. Liu, *Sens. Actuators, B* **2020**, *308*, 127718.
[29] G. Buoli Comani, R. Panceri, M. Dinelli, A. Biondi, C. Mancuso, R. Meneveri, D. Barisani, *Genes Nutr.* **2015**, *10*, 32.
[30] M. Moccia, A. Antonacci, M. Saviano, V. Caratelli, F. Arduini, V. Scognamiglio, *Trends Anal. Chem.* **2020**, *132*, 116062.
[31] A. Raiteri, A. Granito, A. Giamperoli, T. Catenaro, G. Negrini, F. Tovoli, *World J. Gastroenterol.* **2022**, *28*, 154.
[32] G. F. Longstreth, W. G. Thompson, W. D. Chey, L. A. Houghton, F. Mearin, R. C. Spiller, *Gastroenterology* **2006**, *130*, 1480.
[33] E. F. Verdu, D. Armstrong, J. A. Murray, *Am. J. Gastroenterol.* **2009**, *104*, 1587.
[34] F. Ricci, R. Y. Lai, A. J. Heeger, K. W. Plaxco, J. J. Sumner, *Langmuir* **2007**, *23*, 6827.
[35] http://www.admin.ox.ac.uk/uohs/policies-guidance/blood/. (accessed: December 2021).
[36] M. Moccia, V. Caratelli, S. Cinti, B. Pede, C. Avitabile, M. Saviano, A. L. Imbriani, D. Moscone, F. Arduini, *Biosens. Bioelectron.* **2020**, *165*, 112371.
[37] G. Oliviero, S. D'Errico, B. Pinto, F. Nici, P. Dardano, I. Rea, L. De Stefano, L. Mayol, G. Piccialli, N. Borbone, *ChemistryOpen* **2017**, *6*, 599.
[38] S. Cinti, E. Proietti, F. Casotto, D. Moscone, F. Arduini, *Anal. Chem.* **2018**, *90*, 13680.
[39] D. A. Antonioli, *Mod. Pathol.* **2003**, *16*, 342.
[40] S. D. Keighley, P. Estrela, P. Li, P. Migliorato, *Biosens. Bioelectron.* **2008**, *24*, 906.

 © 2022 The Authors. Advanced NanoBiomed Research published by Wiley-VCH GmbH

[41] S. Hassani, M. R. Akmal, A. Salek-Maghsoudi, S. Rahmani, M. R. Ganjali, P. Norouzi, M. Abdollahi, *Biosens. Bioelectron.* **2018**, *120*, 122.
[42] S. Kennedy, N. Oswald, *PCR Troubleshooting and Optimization: The Essential Guide*, Caister Academic Press, Norfolk, UK **2011**.
[43] J. Kuang, X. Yan, A. J. Genders, C. Granata, D. J. Bishop, *PLoS One* **2018**, *13*, e0196438.
[44] M. Filion, *Quantitative Real-Time PCR In Applied Microbiology*, Caister Academic Press, Norfolk, UK **2012**.
[45] K. J. Livak, T. D. Schmittgen, *Methods* **2001**, *25*, 402.
[46] C. Avitabile, L. Moggio, L. D. D'Andrea, C. Pedone, A. Romanelli, *Tetrahedron Lett.* **2010**, *51*, 3716.
[47] S. Cinti, S. Politi, D. Moscone, G. Palleschi, F. Arduini, *Electroanalysis* **2014**, *26*, 931.

 © 2022 The Authors. Advanced NanoBiomed Research published by Wiley-VCH GmbH